1521-009X/12/4008-1628–1640$25.00
DRUG METABOLISM AND DISPOSITION
DMD 40:1628–1640, 2012

Vol. 40, No. 8
45641/3781342

Identification of the *ortho*-Benzoquinone Intermediate of 5-*O*-Caffeoylquinic Acid In Vitro and In Vivo: Comparison of Bioactivation under Normal and Pathological Situations[S]

Cen Xie, Dafang Zhong, and Xiaoyan Chen

Center for Drug Metabolism and Pharmacokinetics, Shanghai Institute of Materia Medica, Chinese Academy of Sciences, Shanghai, China

Received March 12, 2012; accepted May 2, 2012

ABSTRACT:

5-*O*-Caffeoylquinic acid (5-CQA) is one of the major bioactive ingredients in some Chinese herbal injections. Occasional anaphylaxis has been reported for these injections during their clinical use, possibly caused by reactive metabolites of 5-CQA. This study aimed at characterizing the bioactivation pathway(s) of 5-CQA and the metabolic enzyme(s) involved. After incubating 5-CQA with GSH and NADPH-supplemented human liver microsomes, two types of GSH conjugates were characterized: one was M1-1 from the 1,4-addition of GSH to *ortho*-benzoquinone intermediate; the other was M2-1 and M2-2 from the 1,4-addition of GSH directly to the α,β-unsaturated carbonyl group of the parent. The formation of M1-1 was cytochrome P450 (P450)-mediated, with 3A4 and 2E1 as the principal catalyzing enzymes, whereas the formation of M2-1 and M2-2 was independent of NADPH and could be accelerated by cytosolic glutathione transferase. In the presence of cumene hydroperoxide, M1-1 formation increased 6-fold, indicating that 5-CQA can also be bioactivated by P450 peroxidase under oxidizing conditions. Furthermore, M1-1 could be formed by myeloperoxidase in activated human leukocytes, implying that 5-CQA bioactivation is more likely to occur under inflammatory conditions. This finding was supported by experiments on lipopolysaccharide-induced inflammatory rats, where a greater amount of M1-1 was detected. In *S*-adenosyl methionine- and GSH-supplemented human S9 incubations, M1-1 formation decreased by 80% but increased after tolcapone-inhibited catechol-*O*-methyltransferase (COMT) activity. In summary, the high reactivities of the *ortho*-benzoquinone metabolite and α,β-unsaturated carbonyl group of 5-CQA to nucleophiles have been demonstrated. Different pathological situations and COMT activities in patients may alter the bioactivation extent of 5-CQA.

Introduction

Chlorogenic acids are a family of esters formed between *trans*-cinnamic acids and D-(−)-quinic acid. The most widely occurring chlorogenic acid in dietary plants and medicinal herbs is 5-*O*-caffeoylquinic acid [(1*S*,3*R*,4*R*,5*R*)-3-{[(2*Z*)-3-(3,4-dihydroxyphenyl)prop-2-enoyl]oxy}-1,4,5-trihydroxycyclohexanecarboxylic acid; 5-CQA] (Clifford, 2000). It has received much attention in recent years due to its multiple pharmacological properties, such as anti-inflammatory, antioxidant, analgesic, antipyretic, and anticarcinogenic effects (Shibata et al., 1999; Jiang et al., 2000; dos Santos et al., 2006).

Some Chinese herbal injections, such as Shuang-Huang-Lian, Yin-Zhi-Huang, Qing-Kai-Ling, Mai-Luo-Ning, and Xiao-Ai-Ping, are widely used in China to treat common colds, upper respiratory tract infections, cardiovascular diseases, and cancer. However, increasing adverse drug reactions during their clinical use have been reported. Itchy skin, exanthema, asthma, diarrhea, and vomiting are frequently documented. Even severe liver or kidney injury, allergic shock, and fatality are also observed (Ji et al., 2009). 5-CQA is one of the major bioactive ingredients of these injections, and its daily intravenous dosage is from 1 to 45 mg (Zhang et al., 2008, 2009). Several studies have shown that 5-CQA can induce allergic response in humans and rats, as well as liver and kidney injuries in dogs (Freedman et al., 1961; Bariana et al., 1965; Li et al., 2010; Zhang et al., 2010). The potential risks to human health posed by herbal injections containing 5-CQA need to be evaluated further.

The 5-CQA molecule has a catechol and an α,β-unsaturated carbonyl group. Therefore, we speculated that 5-CQA might undergo

This work was supported by the National Natural Science Foundation of China [Grant 81173115]; and the National Basic Research Program of China [Grant 2009CB930300].

Article, publication date, and citation information can be found at http://dmd.aspetjournals.org.

http://dx.doi.org/10.1124/dmd.112.045641.

[S] The online version of this article (available at http://dmd.aspetjournals.org) contains supplemental material.

ABBREVIATIONS: 5-CQA, 5-*O*-caffeoylquinic acid; P450, cytochrome P450; HLM, human liver microsomes; 3-CQA, 3-*O*-caffeoylquinic acid; 4-CQA, 4-*O*-caffeoylquinic acid; CHP, cumene hydroperoxide; MPO, myeloperoxidase; PMA, phorbol 12-myristate 13-acetate; SAM, *S*-adenosylmethionine; ABT, 1-aminobenzotriazole; LPS, lipopolysaccharides; HPLC, high-performance liquid chromatography; UPLC, ultraperformance liquid chromatography; Q-TOF, quadrupole time-of-flight; MS, mass spectrometry; ES, electrospray ionization; CE, collision energy; PBS, phosphate-buffered saline; 7′-SG-5-CQA, 7′-*S*-glutathionyl-5-*O*-caffeoylquinic acid; COMT, catechol-*O*-methyltransferase; 2′-SG-5-CQA, 2′-*S*-glutathionyl-5-*O*-caffeoylquinic acid; GST, glutathione transferase; 5-FQA, 5-*O*-feruloylquinic acid; 5-iFQA, 5-*O*-isoferuloylquinic acid; 4-FQA, 4-*O*-feruloylquinic acid.

metablism to form reactive metabolites and cause adverse effects to human health. Previous studies have pointed out that 5-CQA can be metabolically activated by cytochrome P450 (P450) enzymes, horseradish peroxidase/H_2O_2, and tyrosinase/O_2 to form a cytotoxic quinone intermediate (Moridani et al., 2001, 2002), but these works did not characterize the reactive metabolite(s). Our preliminary study has also shown that 5-CQA underwent extensive metabolism in rats, and the predominant metabolites in bile were GSH conjugates (Xie et al., 2011b). Hence, providing insight into the nature of the reactive intermediates of 5-CQA is important. Furthermore, investigating the impact of different pathological conditions in patients on the bioactivation of 5-CQA is equally vital to understand the potential links between 5-CQA and its toxicity.

In light of these concerns, the objectives of the present study were to 1) elucidate the in vitro metabolic activation of 5-CQA in human liver microsomes (HLM), S9 fractions, and leukocytes, and characterize the structures of reactive metabolite(s); 2) identify the metabolic enzymes involved in the bioactivation of 5-CQA; and 3) explore the fate of 5-CQA in oxidizing and inflammatory environments that are often encountered in therapeutic settings.

Materials and Methods

Materials. The following chemicals were purchased from Sigma-Aldrich (St. Louis, MO): 5-CQA (analytical grade, >95% pure), 3-*O*-caffeoylquinic acid (3-CQA; analytical grade, >95% pure), 4-*O*-caffeoylquinic acid (4-CQA; analytical grade, >95% pure), GSH, sodium nitrite, NADPH, α-naphthoflavone, sulfaphenazole, ticlopidine, quinidine, chlormethiazole, ketoconazole, cumene hydroperoxide (CHP), Ficoll solution, myeloperoxidase (MPO; from human leukocyte, >50 units/mg protein), H_2O_2 (30 wt% in H_2O), phorbol 12-myristate 13-acetate (PMA), *S*-adenosyl methionine (SAM), 1-aminobenzotriazole (ABT), lipopolysaccharides (LPS) from *Escherichia coli* 0111:B4, and leucine enkephalin. Tolcapone (>99% pure) was obtained from TLC PharmaChem Inc. (Vaughan, Ontario, Canada). HLM (pooled from 50 donors), human liver S9 fractions (pooled from 150 donors), human liver cytosol (pooled from 50 donors), and recombinant P450 enzymes (P450 1A2, 2C9, 2C19, 2D6, 2E1, and 3A4) were purchased from BD Gentest (Woburn, MA). All other reagents and solvents were either analytical or high-performance liquid chromatography (HPLC) grade.

Instrumentation. Metabolite profiling was performed on an ACQUITY ultraperformance liquid chromatography (UPLC) system coupled with a quadrupole-time-of-flight (Q-TOF) mass spectrometry (MS) instrument (UPLC/Synapt Q-TOF MS; Waters, Milford, MA) with an electrospray ionization (ES) source.

Separation was achieved on a Phenomenex Luna-C18 column (150 × 4.6 mm i.d., 5 μm; Phenomenex, Torrance, CA) protected by a SecurityGuard C18 column (4.0 × 4.6 mm i.d., 5 μm; Phenomenex). The mobile phase was a mixture of 0.1% formic acid (A) and methanol (B). The gradient elution involved 10% B maintained for 3 min, a 12-min linear gradient from 10 to 40% B maintained for 1 min, an 8-min linear increase to 80% B, and finally a decrease to 10% B to equilibrate the column. The flow rate was 0.7 ml/min. The UPLC effluent was directed to waste through a diverter value for the first 3 min after sample injection, and then to the ionization source.

MS detection was conducted in the ES− mode. The major operating parameters for the Q-TOF MS were set as follows: capillary voltage, 2.8 kV; cone voltage, 40 V; source temperature, 120°C; desolvation temperature, 450°C; collision gas, argon; desolvation gas (nitrogen) flow rate, 800 l/h; data acquisition range, *m/z* 80 to 1300 Da; and data format, centroid. The lock mass solution was leucine enkephalin with a reference mass at *m/z* 554.2615, which was infused at 5 μl/min. Data were acquired under the MS^E mode, in which two separate scan functions were programmed with independently low- and high-collision energies (CEs). The mass spectrometer switched rapidly between these two functions during data acquisition. As a result, information on intact precursor ions as well as fragment ions was obtained from one LC run. In this set, one scan function used a low CE setting (5 V of trap CE and 3 V of transfer CE) and the other scan function used a high CE setting (ramped trap CE from 10 V to 20 V and 15 V of transfer CE).

Data analysis and instrument control were performed using the MassLynx 4.1 software (Waters). Data were processed using a subroutine of the MassLynx software, MetaboLynx, which uses mass defect filtering and the dealkylation tool to identify metabolite ions.

Human Liver Microsomal Metabolism. A stock solution of 5-CQA was prepared in methanol. 5-CQA (500 μM) was mixed with HLM (1 mg/ml), GSH (5 mM), magnesium chloride (5 mM), and phosphate-buffered saline (PBS; 100 mM, pH 7.4) in a final volume of 250 μl. The final concentration of methanol in the incubation is 0.1%. The mixture was preincubated at 37°C for 3 min and then initiated by adding NADPH (final concentration of 1 mM). Control samples with no NADPH, no GSH, no enzyme, or no substrate were also prepared. The reaction was terminated after 60 min of incubation by adding two volumes of ice-cold acetonitrile. The resulting mixture was centrifuged at 11,000*g* (4°C) to precipitate the proteins. A 200-μl aliquot of supernatant was collected and evaporated to dryness under a stream of nitrogen at 40°C, and then reconstituted in 100 μl of mobile phase (water/methanol/formic acid, 90:10:0.1, v/v/v). A 10-μl aliquot of the reconstituted solution was injected into the UPLC/Q-TOF MS system for analysis. Each incubation was performed in duplicate.

Recombinant Human P450 Phenotyping. The incubation conditions were set similarly to those of the microsomal incubations, except that the microsomes were substituted with recombinant cDNA-expressed P450s 1A2, 2C9, 2C19, 2D6, 2E1, and 3A4. The concentrations of the P450 enzymes were 50 nM. Each incubation was performed in triplicate. A total normalized rate method was applied to determine the involvement of P450(s) in the bioactivation of 5-CQA. The rates of metabolite formation in individual incubations with recombinant P450 enzymes were multiplied by the mean specific content of the corresponding P450 enzyme in HLM to obtain the "normalized" reaction rates for each enzyme (Rodrigues, 1999).

P450 Inhibition by Chemical Inhibitors. To investigate the specific P450 enzyme(s) primarily responsible for the formation of reactive metabolites, a total of six P450-specific inhibitors were tested. These inhibitors were α-naphthoflavone (0.1 μM), sulfaphenazole (60 μM), ticlopidine (0.4 μM), quinidine (2.0 μM), chlormethiazole (0.1 μM), and ketoconazole (1.0 μM) for P450 1A2, 2C9, 2C19, 2D6, 2E1, and 3A4, respectively. The incubation mixtures consisted of 5-CQA (500 μM), HLM (1 mg/ml), GSH (5 mM), inhibitors (various concentrations), magnesium chloride (5 mM), and PBS (100 mM, pH 7.4) in a final volume of 250 μl. Control samples with no chemical inhibitor were also prepared. Incubations were started by adding NADPH (final concentration of 1 mM), and quenched by adding two volumes of ice-cold acetonitrile after 60 min. The samples were then prepared as described above. The production of GSH conjugates was monitored and quantitated by UPLC/Q-TOF MS. Each incubation was performed in triplicate. A comparison relative to the controls was made, and P450 activity was expressed as the percentage of control activity.

Human Liver Cytosol Metabolism. The incubation mixtures contained 5-CQA (500 μM), GSH (5 mM), and PBS in a final volume of 200 μl. After preincubation at 37°C for 3 min, the reactions were initiated by adding human liver cytosol (final concentration of 1 mg/ml) and then terminated by adding two volumes of ice-cold acetonitrile after 90 min. The samples were then prepared as described above. Control samples with no human liver cytosol were also prepared. Each incubation was performed in duplicate.

Effect of CHP on 5-CQA Bioactivation. The incubation conditions were equivalent to the microsomal incubations except that CHP (1 mM) was used in place of NADPH to initiate the reaction. The reactions were terminated after 30 min of incubation. Two control experiments were included, namely, HLM (with NADPH as the cofactor, without CHP) and CHP only (without HLM). The yields of GSH conjugates generated were compared by peak areas.

Human Leukocytes Metabolism. Fresh heparinized whole blood from three healthy male adults was provided by Shanghai Shuguang Hospital (Shanghai, China). The whole blood was first fractionated by centrifugation at 1300*g* for 10 min at room temperature. The lower blood cell layer was then diluted with two volumes of physiological saline (0.9% NaCl) and then laid over the Ficoll solution. The tube was centrifuged at 480*g* for 25 min at room temperature. The interface containing the leukocyte fraction was pipetted and washed three times with Hank's balanced salt solution. The purity of the isolated cells was approximately 95%, and the viability was >95%. The

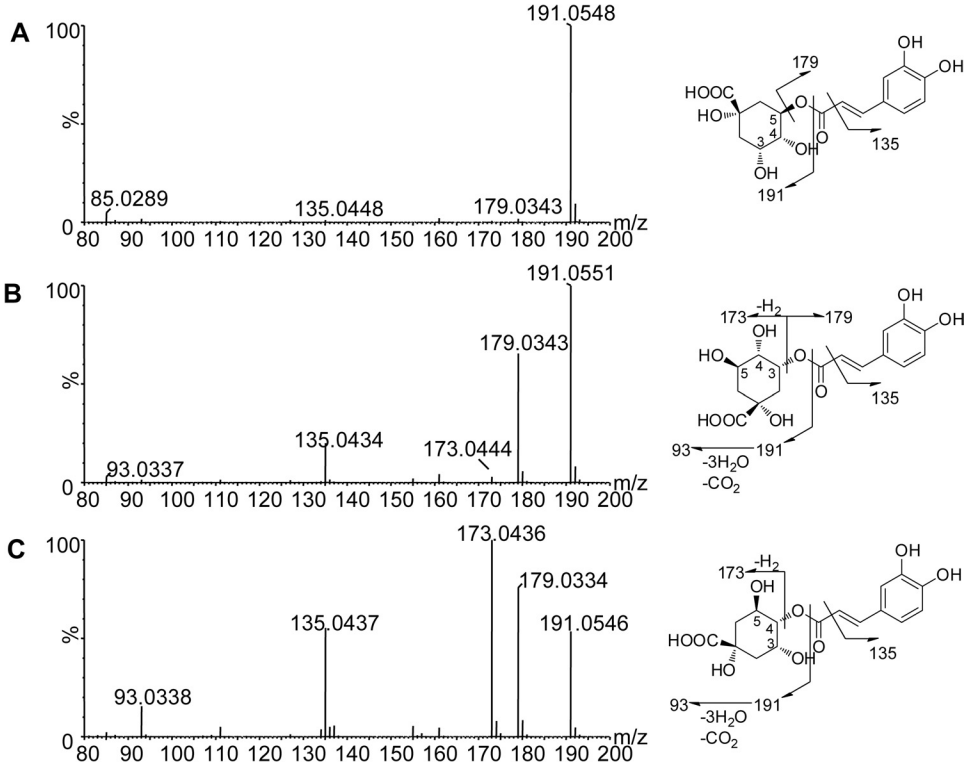

FIG. 1. Q-TOF mass spectra of the standards 5-CQA (A), 3-CQA (B), and 4-CQA (C) under high-collision energy in the ES^- mode.

leukocytes were cultured in Hank's balanced salt solution containing 0.1% human serum albumin for 1 day.

5-CQA (500 μM), GSH (5 mM), and PMA (100 ng/ml) were added to a 200-μl suspension of leukocytes ($\sim 1 \times 10^6$ cells/ml) in Hank's balanced salt solution containing 0.1% human serum albumin. The mixture was incubated at 37°C for 2 h and quenched by adding two volumes of ice-cold acetonitrile. Control samples with no PMA, no GSH, or no substrate were also prepared. The samples were then prepared as described above. Each incubation was performed in duplicate.

Incubations of 5-CQA with MPO. The incubation mixtures contained 5-CQA (500 μM), MPO (6 unit/ml), and GSH (5 mM). PBS (100 mM, pH 7.4) was added to 200 μl. The reactions were initiated by adding H_2O_2 (final concentration of 2 mM) after preincubating at 37°C for 3 min and then terminated by adding two volumes of ice-cold acetonitrile after 15 min. The samples were then prepared as described above. Control samples with no H_2O_2, no GSH, or no substrate were also prepared. Each incubation was performed in duplicate.

Human Liver S9 Fraction Metabolism. The incubation mixtures contained 5-CQA (500 μM), 1 mM NADPH, SAM (500 μM), GSH (5 mM), and magnesium chloride (5 mM). PBS (100 mM, pH 7.4) was added to 300 μl. After preincubation at 37°C for 3 min, the reactions were initiated by adding human liver S9 fractions (2 mg/ml) and then terminated by adding two volumes of ice-cold acetonitrile after 90 min. The samples were then prepared as described above. Control samples with no NADPH, no SAM, no GSH, or no substrate were also prepared. Each incubation was performed in duplicate.

In a separate study, a scaled-up human liver S9 fraction incubation (500 μl) with 5-CQA (1 mM) was performed under similar experimental conditions as described above, but without GSH. After 90 min of incubation, the reaction was terminated by adding two volumes of ice-cold acetonitrile and then centrifuged at 1300*g* for 10 min. The resulting supernatants were evaporated to

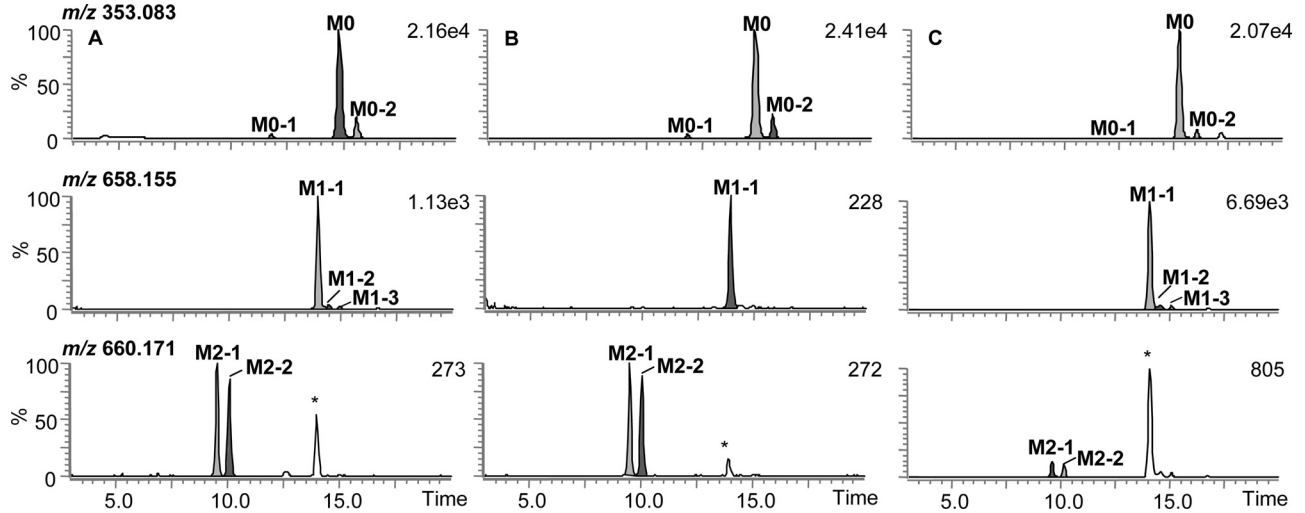

FIG. 2. Extracted ion chromatograms of 5-CQA and its GSH conjugates in HLM incubations: with NADPH and GSH (A), with GSH but without NADPH (B), and with CHP and GSH (C). The asterisk (*) indicates an isotopic peak of M1-1.

dryness under a stream of nitrogen at 40°C, reconstituted in 100 μl of mobile phase (water/methanol/formic acid, 90:10:0.1, v/v/v), and then subjected to UPLC separation. Fractions with retentions times of 18.3 (M6-1) and 19.1 (M6-2) min were collected and pooled. The pooled fractions were halved and evaporated to dryness under a stream of nitrogen at 40°C. The crude mixture of M6-1 and M6-2 was used without further purification and incubated with human liver S9 fractions (2 mg/ml) in the presence or absence of GSH (5 mM). The synthetic 7′-*S*-glutathionyl-5-*O*-caffeoylquinic acid (7′-SG-5-CQA; 500 μM) was also incubated with human liver S9 fractions (2 mg/ml), SAM (500 μM), and PBS (100 mM, pH 7.4).

A specific catechol-*O*-methyltransferase (COMT) inhibitor, tolcapone (5 μM), was used to investigate the impact of O-methylation on 5-CQA bioactivation. The mixture of tolcapone, human liver S9 fractions, NADPH, and magnesium chloride was preincubated at 37°C for 15 min. 5-CQA, SAM, and GSH were then added, and the resulting mixture was incubated for 90 min.

Animal Experiments. Male Wistar rats (200 ± 20 g) were obtained from Shanghai SLAC Laboratory Animal Co., Ltd. (Shanghai, China). The rats were randomly divided into four groups (three rats per group) and housed in four cages, with free access to food and water. 5-CQA dissolved in physiological saline was administered to each rat by intravenous injection (5 ml/kg) via a tail vein at a dose of 11 mg/kg (approximately 2 times the recommended intravenous dose in humans). In group I, rats were given intravenous injections of 5-CQA only. In group II, rats were treated orally with tolcapone (10 mg/kg) 30 min before 5-CQA administration. In group III, rats were given 100 mg/kg ABT i.p. simultaneously with 10 mg/kg tolcapone p.o. 30 min before the

TABLE 1

Metabolite data for 5-CQA in human liver microsomes, liver S9 fractions, cytosol, leukocytes, and myeloperoxidase incubations

No.	Description	Retention Time	Formula	Calculated Mass	Measured Mass	Fragment Ions	Matrices
		min		$[M + H]^+$			
M0	5-CQA	15.0	$C_{16}H_{18}O_9$	353.083	353.085	191.053, 179.033, 173.044, 135.043, 93.034	HLM, cytosol, S9, leukocytes, MPO
M0-1	3-CQA	11.9	$C_{16}H_{18}O_9$	353.083	353.088	191.055, 179.034, 173.044, 135.043	HLM, cytosol, S9, leukocytes, MPO
M0-2	4-CQA	15.7	$C_{16}H_{18}O_9$	353.083	353.085	191.055, 179.033, 173.044, 135.044, 93.034	HLM, cytosol, S9, leukocytes, MPO
M1-1	2′-SG-5-CQA	13.8	$C_{26}H_{33}N_3O_{15}S$	658.155	658.151	466.092, 385.059, 306.078, 272.086, 254.075, 191.055	HLM, cytosol, S9, leukocytes, MPO
M1-2	2′-SG-4-CQA	14.4	$C_{26}H_{33}N_3O_{15}S$	658.155	658.154	466.093, 385.059, 272.088, 254.073, 191.054, 173.039	HLM, leukocytes, MPO
M1-3	5′-SG-5-CQA	14.8	$C_{26}H_{33}N_3O_{15}S$	658.155	658.152	466.090, 385.056, 306.074, 272.082, 254.075, 191.053	HLM, leukocytes, MPO
M1-4	2′-SG-3-CQA	11.0	$C_{26}H_{33}N_3O_{15}S$	658.155	658.152	466.092, 385.056, 272.093, 254.087, 191.053, 179.052	Leukocytes
M2-1	7′-SG-5-CQA	9.3	$C_{26}H_{35}N_3O_{15}S$	660.171	660.172	353.081, 306.072, 272.086, 254.075, 191.053	HLM, cytosol, S9, leukocytes, MPO
M2-2	7′-SG-5-CQA	9.8	$C_{26}H_{35}N_3O_{15}S$	660.171	660.172	353.083, 306.075, 272.088, 254.074, 191.057	HLM, cytosol, S9, leukocytes, MPO
M2-3	7′-*S*-glutathionyl-3-*O*-caffeoylquinic acid	7.2	$C_{26}H_{35}N_3O_{15}S$	660.171	660.169	353.086, 306.074, 272.087, 254.077, 191.053, 179.033	Cytosol, leukocytes
M2-4	7′-*S*-glutathionyl-4-*O*-caffeoylquinic acid	9.0	$C_{26}H_{35}N_3O_{15}S$	660.171	660.170	353.085, 306.076, 272.087, 254.075, 191.053, 179.033, 173.043	Cytosol, leukocytes
M3	2′,5′-di-*S*-glutathionyl-5-*O*-caffeoylquinic acid	13.6	$C_{36}H_{48}N_6O_{21}S_2$	963.227	963.240	834.196, 771.171, 690.131, 498.066, 417.028, 369.022, 272.087, 224.964, 191.049	MPO
M4-1	2′,7′-di-*S*-glutathionyl-5-*O*-caffeoylquinic acid	9.4	$C_{36}H_{50}N_6O_{21}S_2$	965.240	965.250		MPO
M4-2	2′,7′-di-*S*-glutathionyl-5-*O*-caffeoylquinic acid	10.1	$C_{36}H_{50}N_6O_{21}S_2$	965.240	965.247		MPO
M5	2′,5′,6′-tri-*S*-glutathionyl-5-*O*-caffeoylquinic acid	9.1	$C_{46}H_{63}N_9O_{27}S_3$	1268.299	1268.317	1139.276, 995.214, 961.229, 803.138, 688.120, 530.037, 415.016, 272.083, 256.934, 191.050	MPO
M6-1	5-FQA	18.3	$C_{17}H_{20}O_9$	367.103	367.102	191.053, 173.043	S9
M6-2	5-iFQA	19.1	$C_{17}H_{20}O_9$	367.103	367.109	193.051, 173.043, 111.046	S9
M6-3	4-iFQA	19.5	$C_{17}H_{20}O_9$	367.103	367.106	193.052, 191.054, 173.043	S9
M7-1	7′-*S*-glutathionyl-5-*O*-feruloylquinic acid	11.3	$C_{27}H_{37}N_3O_{15}S$	674.187	674.196	367.111, 306.084, 272.087, 254.076, 191.057	S9
M7-2	7′-*S*-glutathionyl-5-*O*-feruloylquinic acid	11.8	$C_{27}H_{37}N_3O_{15}S$	674.187	674.198	367.093, 306.078, 272.087, 254.090, 191.056	S9
M7-3	7′-*S*-glutathionyl-5-*O*-isoferuloylquinic acid	12.7	$C_{27}H_{37}N_3O_{15}S$	674.187	674.188	367.108, 306.079, 272.093, 254.077, 173.048	S9
M7-4	7′-*S*-glutathionyl-5-*O*-isoferuloylquinic acid	13.3	$C_{27}H_{37}N_3O_{15}S$	674.187	674.195	367.113, 306.079, 272.095, 254.086, 173.051	S9

injection of 5-CQA. In group IV, rats were treated intravenously with LPS (7.4×10^6 EU/kg) 2 h before 5-CQA administration. After light anesthesia with ether, approximately 300 μl of blood samples were serially collected from each animal into heparinized tubes by puncturing the retro-orbital sinus at predose (0 h) and 15 min postdose. Approximately 150 μl of plasma was immediately obtained from each sample by centrifugation at 11,000*g* (4°C) for 5 min and then mixed with a 5-μl aliquot of 4 M H_3PO_4 to stabilize the metabolites. The samples were pooled according to predetermined time points and precipitated with acetonitrile. The precipitated samples were vortex-mixed and then centrifuged at 11,000*g* for 5 min at 4°C. A 200-μl aliquot of supernatant was evaporated to dryness under a stream of nitrogen at 40°C and then reconstituted in 100 μl of the initial mobile phase. A 10-μl aliquot of the reconstituted solution was injected into the UPLC/Q-TOF MS system for analyses.

Results

In the early stages of the in vitro metabolism studies on 5-CQA, intramolecular *ortho*-acyl migration phenomena from 5-CQA to 4-CQA and 3-CQA catalyzed by hydroxide ions were observed (Xie et al., 2011a). The metabolites of 5-CQA containing acyl groups were expected to follow the same isomerization. According to previous reports and our experience (Clifford et al., 2003; Xie et al., 2011a), the acyl isomers of 5-CQA and its metabolites can be distinguished by their chromatographic and characteristic MS fragmentation behaviors. In general, 5-CQA gave a predominant ion at *m/z* 191.053 ([quinic acid − H]$^-$) in the high CE spectrum, which was formed by the cleavage of the ester bond (Fig. 1A). 3-CQA also showed the base peak at *m/z* 191.053; however, a strong key ion was observed at *m/z* 179.034 ([caffeic acid − H]$^-$) formed by the cleavage of the alkyl C–O bond adjacent to the ester (Fig. 1B). 4-CQA exhibited the base peak ion at *m/z* 173.044 ([quinic acid − H_2O − H]$^-$), which was a characteristic ion for the isomer with caffeic acid substituted at position 4, and formed by the cleavage of the alkyl C–O bond adjacent to the ester (Fig. 1C).

Bioactivation of 5-CQA in HLM. In the incubations of 5-CQA with NADPH-supplemented HLM, no oxidative metabolite was detected apart from the two acyl-isomers [3-CQA (M0-1) and 4-CQA (M0-2)]. When the trapping agent GSH was included in the incubations, a total of five GSH conjugates were detected (M1-1, M1-2, M1-3, M2-1, and M2-2). Their structures were characterized by high-resolution MS and NMR spectral data. Representative UPLC/Q-TOF MS chromatograms of the HLM incubations with or without NADPH are illustrated in Fig. 2, A and B, respectively. Table 1 summarizes the detailed information on these metabolites identified in HLM, including the LC retention times, chemical formulae, accurate masses, and characteristic fragment ions.

The LC retention times of M1-1, M1-2, and M1-3 were 13.8, 14.4, and 14.8 min, respectively. They displayed deprotonated molecules at *m/z* 658.155, which was 305.072 Da higher than that of the parent drug. This finding suggested the addition of one molecule of GSH to 5-CQA and the removal of two hydrogen atoms. Upon further fragmentation, M1-1 and M1-3 showed identical product ions at *m/z* 466.092, 385.059, 306.078, 272.086, 254.075, and 191.055 (Fig. 3A). The appearance of [quinic acid − H]$^-$ ion at *m/z* 191.055 without obvious fragment ions at *m/z* 179.033 and 173.044 supported the assumption that they were derived from 5-CQA rather than its acyl-isomers. The base peak ion at *m/z* 385.059 was generated via the cleavage of the C–S bond of the glutathionyl moiety, and its occurrence suggested the presence of aromatic-orientated thioether motif in the GSH conjugates referring to MS fragmentation properties of the reported aromatic-orientated thioether GSH conjugates (Yan et al., 2008; Deng et al., 2010). The fragment ions at *m/z* 466.092 and 191.055 were formed via the cleavage of the ester bond. The fragment ions at *m/z* 306.078 and 272.096 corresponded to deprotonated GSH and γ-glutamyl-dehydroalanyl-glycine, respectively. The definitive structures of M1-1 and M1-3 cannot be determined based only on MS data. To assign further the region of modification in the M1-1 molecule, this metabolite was chemically synthesized according to a published nitrite-promoted oxidation method (Panzella et al., 2003) and was purified by an LC-6AD semipreparative HPLC system (Shimadzu Corp., Kyoto, Japan) with a reversed C18 column (isobaric eluting with CH_3CN/water/formic acid, 12:88:0.5, v/v/v). The ^{1}H

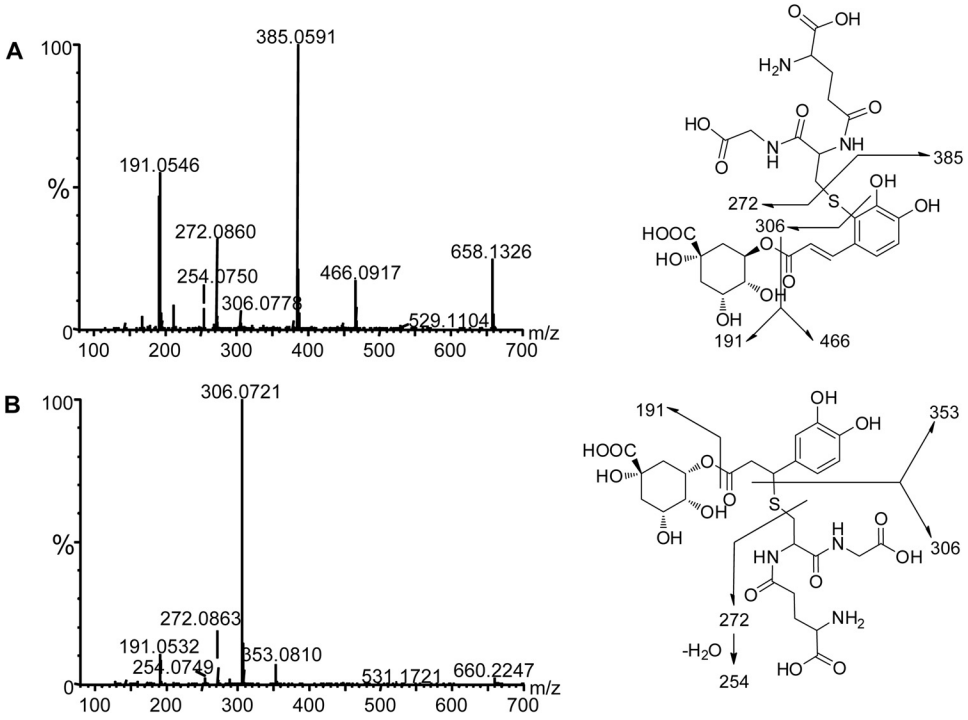

FIG. 3. Q-TOF mass spectra of GSH conjugates M1-1 (A) and M2-1 (B) under high-collision energy in the ES$^-$ mode.

TABLE 2

Peak areas of major GSH conjugates in human liver microsomes, liver S9 fractions, leukocytes, and myeloperoxidase incubations

No.	Liver Microsomes			Leukocytes		Myeloperoxidase		Liver S9 Fractions		
	+ NADPH	− NADPH	+ CHP	+ PMA	− PMA	+ H_2O_2	−H_2O_2	− SAM + GSH	+ SAM + GSH	+ SAM + GSH + Tolcapone
M1-1	204	39.5	1245	117	30.7	713	5.3	87.2	17.5	73.3
M2-1	35.8	35.7	20.8	216	157	11.2	28.4	314	584	369
M2-2	31.3	31.2	19.5	148	112	8.6	16.4	243	486	286

NMR spectrum (400 MHz, in CD_3OD) is presented in Supplemental Fig. S1. The chemical shifts and *J*-couplings of M1-1 were consistent with those reported for 2′-*S*-glutathionyl-5-caffeoylquinic acid (2′-SG-5-CQA) in literature (Panzella et al., 2003). Taken together, the MS and NMR data identified M1-1 as a 5-CQA-derived GSH conjugate with the glutathionyl moiety attached to the C-2′ position of the corresponding *ortho*-benzoquinone intermediate. The three carbons of the *ortho*-benzoquinone of 5-CQA have different electrophilicities in a decreasing order of C-2′ > C-5′ > C-6′ (Panzella et al., 2003). Based on this estimate, M1-3 was tentatively assigned as a 5-CQA-derived GSH conjugate with the glutathionyl moiety attached to the C-5′ position. M1-2 shared similar fragment ions with M1-1, except that an ion at *m/z* 173.039 was observed, indicating that M1-2 was a GSH conjugate derived from 4-CQA at the C-2′ position.

The LC retention times of M2-1 and M2-2 were 9.3 and 9.8 min, respectively. They possessed protonated molecules at *m/z* 660.171, which was 307.088 Da higher than that of the parent drug. This finding can indicate the introduction of one molecule of GSH to 5-CQA. The presence of [quinic acid − H]$^-$ ion at *m/z* 191.055 rather than at *m/z* 179.033 and 173.044 in the high CE spectra (Fig. 3B) supported the possibility that M2-1 and M2-2 were derived from 5-CQA but not from its acyl isomers. In the high CE spectra of M2-1 and M2-2, the predominant product ion was at *m/z* 306.072 (deprotonated glutathionyl moiety), which arose from a neutral loss of 5-CQA molecule (354.099 Da). Other product ions resulting from the sequential fragmentation of the glutathionyl moiety at *m/z* 272.086 and 254.075 with low abundances were also observed. The facile neutral losses of intact 5-CQA molecules from the conjugates indicated that M2-1 and M2-2 were two alkyl-orientated GSH conjugates (Yan et al., 2008; Deng et al., 2010). To confirm further the structural assignment, an attempt to synthesize the two metabolites was made. 5-CQA and GSH were dissolved in PBS and then stirred at 50°C for 20 h. The reaction mixture was concentrated under reduced pressure and further purified using an LC-6AD semipreparative HPLC system with a reversed C18 column (isobaric eluting with CH_3CN/water/formic acid, 10:90:0.5, v/v/v). Unfortunately, the high hydrophilicity of the two GSH conjugates conferred difficulty in gaining a pure product. Thus, a mixture of GSH conjugates (M2-1 and M2-2) was subjected to ^{1}H NMR analysis (400 MHz, in CD_3OD) to determine the site where GSH addition takes place. Compared with the ^{1}H NMR spectrum of the parent 5-CQA, two vinyl proton signals at 6.72 ppm (d, J = 8.2 Hz, 1H) and 7.50 ppm (d, J = 15.9 Hz, 1H) were missing in the ^{1}H NMR spectrum of the metabolite mixture (Supplemental Fig. S2). M2-1 and M2-2 were most likely formed by the 1,4-addition of one GSH to the α,β-unsaturated carbonyl group at C-7′ to form 7′-SG-5-CQA. After the addition, a new chiral center was generated. M2-1 and M2-2 are a pair of diastereomeric conjugates; thus, two peaks were observed in the chromatogram.

Among the GSH conjugates, M1-1 was the most abundant based on the peak areas. The formation of the exocyclic GSH conjugates M2-1 and M2-2 was NADPH independent. When only 5-CQA and GSH were incubated in the HLM, trace amounts of the ring GSH conjugates M1-1 to M1-3 were detected, but their yields significantly increased by almost five times after the incorporation of NADPH (Table 2). This finding indicated that P450s can accelerate 5-CQA bioactivation to *ortho*-benzoquinone.

P450 Enzymes Responsible for the Bioactivation of 5-CQA. To determine which P450 enzyme(s) preferentially oxidize catechol to the *ortho*-benzoquinone intermediate, the formation of the main GSH conjugate M1-1 was investigated in different recombinant individual human P450 enzymes: 1A2, 2C9, 2C19, 2D6, 2E1, and 3A4. Each P450 enzyme tested had some capability of bioactivating 5-CQA. However, after normalization for the relative hepatic abundance of the P450 enzymes (Fig. 4A), 3A4 and 2E1 were identified as the two principal catalyzing enzymes exhibiting the highest efficiencies.

To further determine the primary enzyme(s), α-naphthoflavone (P450 1A2 inhibitor), sulfaphenazole (P450 2C9 inhibitor), ticlopidine (P450 2C19 inhibitor), quinidine (P450 2D6 inhibitor), chlormethiazole (P450 2E1 inhibitor), and ketoconazole (P450 3A4 inhibitor) were used in the inhibition studies to monitor the formation of the conjugate M1-1 in HLM. The yield of M1-1 in HLM was inhibited by up to 65% by ketoconazole and 48% by chlormethiazole, compared with the control (Fig. 4B). No significant inhibition was observed in the HLM in the presence of the other inhibitors. These data confirmed that 3A4 and 2E1 were the two key P450 enzymes bioactivating 5-CQA.

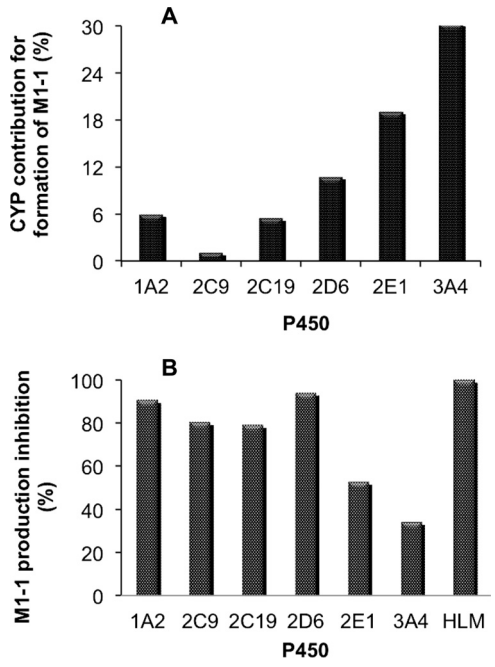

FIG. 4. A, formation of M1-1 in incubations with recombinant human P450 enzymes. The rates of M1-1 formation obtained from individual incubations with recombinant P450 enzymes were multiplied by the mean specific content of the corresponding P450 enzyme in HLM. B, effect of selective P450 inhibitors on the formation of M1-1 in incubations of 5-CQA with HLM. Data are reported as the mean of three separated determinations.

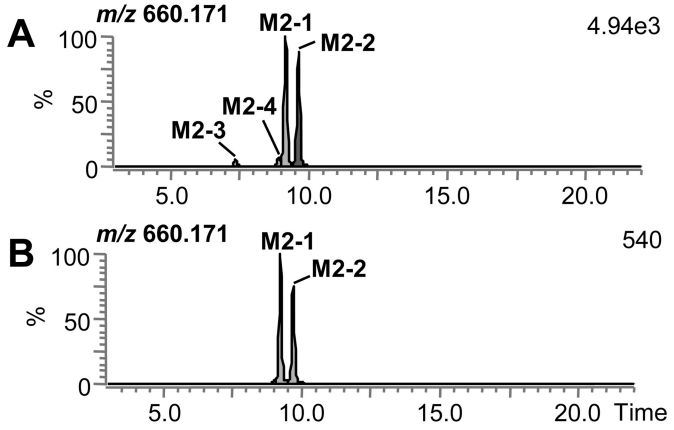

FIG. 5. Extracted ion chromatograms of M2 in human liver cytosol incubations (A) and in buffer (B).

The Role of Glutathione Transferase in the Formation of the Exocyclic GSH Conjugates. To figure out the role of glutathione transferase (GST) in GSH adduction to the α,β-unsaturated carbonyl group, the GSH conjugation of 5-CQA was investigated in buffer, HLM, and human liver cytosol. In buffer, the two exocyclic GSH conjugates (M2-1 and M2-2, *m/z* 660.171) were detected. In the presence of HLM, the yields of M2-1 and M2-2 were similar to those in buffer. In the presence of cytosol, the yields of M2-1 and M2-2 were increased by almost 15 times (Fig. 5). Another two exocyclic GSH conjugates (M2-3 and M2-4, *m/z* 660.171) were also detected. This finding indicated that the cytosolic GST, not microsomal GST, can catalyze the GSH adduction towards the α,β-unsaturated carbonyl group of 5-CQA.

Effect of CHP on the Formation of the Ring GSH Conjugate M1-1. To evaluate the effect of oxidizing conditions on the formation of *ortho*-benzoquinone, CHP was used in the HLM incubation. When 5-CQA was incubated with CHP- and GSH-supplemented HLM, the formation of M1-1 was enhanced six times (Fig. 2C; Table 2), providing evidence that oxidative stress in vivo may accelerate the production of reactive *ortho*-benzoquinone species.

Bioactivation of 5-CQA by Human Leukocytes and MPO. When 5-CQA was incubated with human leukocytes, several metabolites were detected in the presence of PMA and GSH (Fig. 6A). These metabolites were identified as the acyl isomers of 5-CQA (M0-2 and M0-3, *m/z* 353.083), ring GSH conjugates (M1-1, M1-2, M1-3, and M1-4, *m/z* 658.155), and exocyclic GSH conjugates (M2-1, M2-2, M2-3, and M2-4, *m/z* 660.171). With bioactivation by PMA, a 4-fold increase in M1-1 formation was observed in the leukocyte incubations (Table 2).

According to the high CE spectrum, M1-4 was tentatively elucidated as 2′-*S*-glutathionyl-3-*O*-caffeoylquinic acid. Likewise, M2-3 and M2-4 were assigned as 7′-*S*-glutathionyl-3-*O*-caffeoylquinic acid and 7′-*S*-glutathionyl-4-*O*-caffeoylquinic acid, respectively. A previous stability study on 5-CQA in PBS showed that greater acyl migration was induced with a longer incubation period (Xie et al., 2011a). Thus, higher amounts of the acyl-isomerized products of 5-CQA and its metabolites were detected in the leukocyte incubations (incubation time of 2 h) than in other incubations (incubation time of equal to or less than 1 h).

MPO is the most abundant enzyme in leukocytes. Hence, its role in the bioactivation of 5-CQA was investigated. The rapid formation of ring GSH conjugates M1-1 to M1-3 were observed within 15 min of the MPO-mediated incubations (Fig. 7A), and the amount of M1-1 was much greater than that in any other incubation (Table 2). Trace levels of bi- and tri-GSH conjugates (M3, M4-1, M4-2, and M5) were also detected. Information on the metabolites identified in human leukocytes and MPO incubations are listed in Table 1.

M3 with a retention time of 13.6 min exhibited a deprotonated molecule at *m/z* 963.224, which was 305.072 Da higher than that of M1-1, suggesting the addition of the other GSH molecule to M1-1 and the removal of two hydrogen atoms. The fragment ions at *m/z* 690.131 and 417.028 in the high CE spectrum were formed by the sequential cleavage of the glutathionyl C–S bond to lose two γ-glutamyl-dehydroalanyl-glycine groups (−273.105 Da), consistent with the two glutathionyl moieties contained in M3. M5, with a retention time of 9.1 min, showed a deprotonated molecule at *m/z* 1268.299, which was 305.072 Da higher than that of M3, suggesting the addition of another molecule of GSH to M3 and the removal of two hydrogen atoms. The fragment ions at *m/z* 961.229, 688.120, and 415.016 in the high CE spectrum were formed by successive losses of one glutathionyl group (−307.088 Da) and two γ-glutamyl-dehydroalanyl-glycine groups (−273.109 Da), identical with the three glutathionyl motifs in M5. As mentioned under *Bioactivation of 5-CQA in HLM* in the *Results*, the ring (M1) and exocyclic (M2) GSH conjugates exhibited distinctive fragment characteristics. For M2, the most abundant product ion was

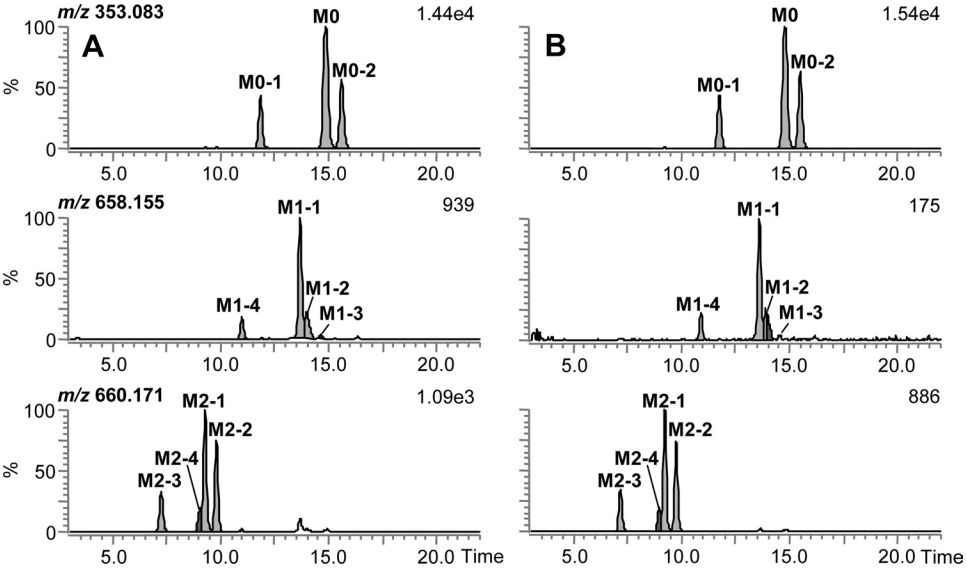

FIG. 6. Extracted ion chromatograms of 5-CQA and its metabolites in human leukocytes incubations: with PMA (A) and without PMA (B).

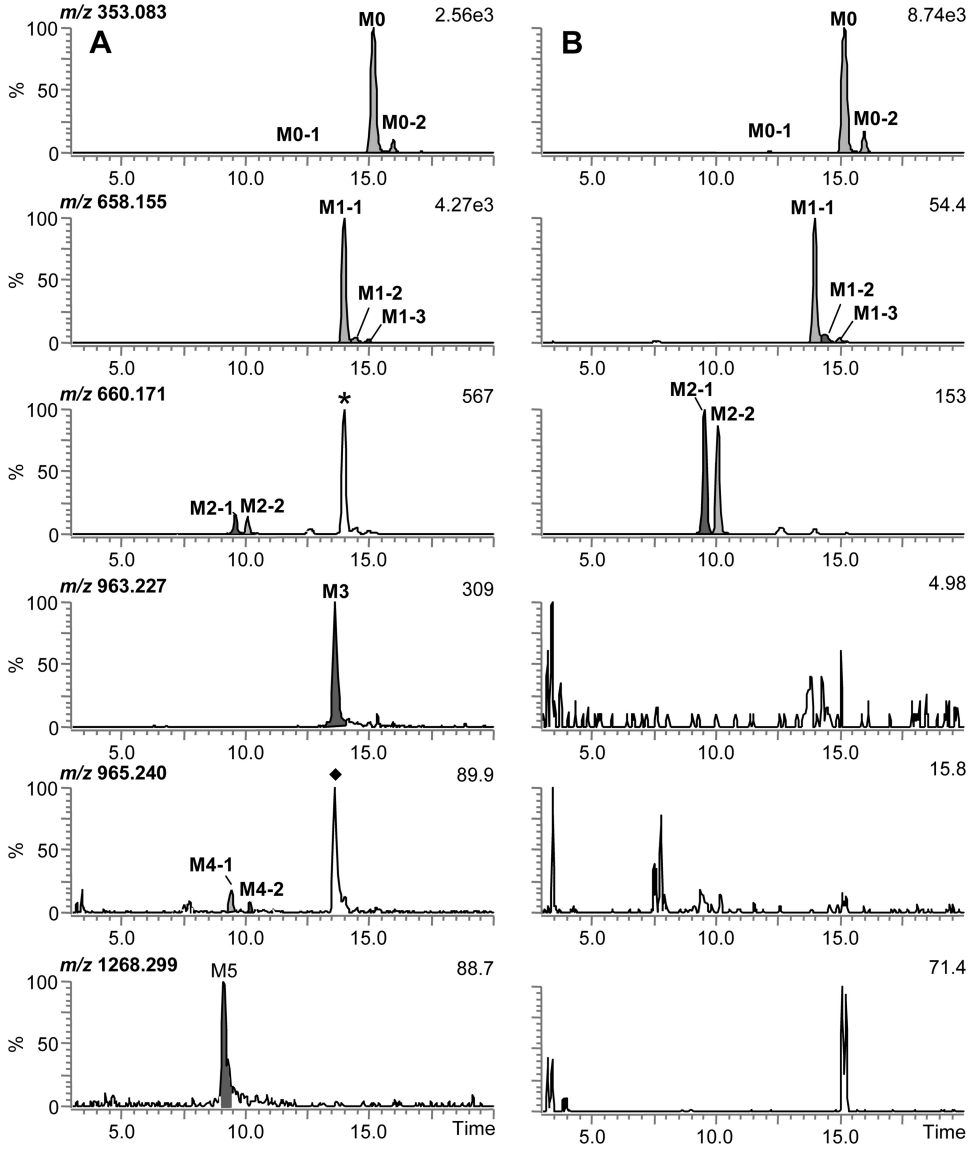

FIG. 7. Extracted ion chromatograms of 5-CQA and its GSH conjugates in MPO incubations: with H_2O_2 (A) and without H_2O_2 (B). The asterisk indicates an isotopic peak of M1-1. The diamond indicates an isotopic peak of M3.

observed at *m/z* 306.072 originating from a GSH moety, whereas for M1, the major fragment ion was at *m/z* 272.096. In the high CE spectra of M3 and M5, they both gave the predominant fragment ion at *m/z* 272.087 rather than *m/z* 306.072, indicative of the ring GSH conjugates. According to the different electrophilicities of the three carbons in *ortho*-benzoquinone, M3 was speculated to be most likely 2′,5′-di-*S*-glutathionyl-5-CQA and M5 was 2′,5′,6′-tri-*S*-glutathionyl-5-CQA.

The LC retention times of M4-1 and M4-2 were 9.4 and 10.1 min, respectively. They displayed deprotonated molecules at *m/z* 965.246, which was 307.089 Da higher than that of M1-1, suggesting the introduction of one molecule of GSH to M1-1. Due to the low amount of these generated metabolites, no high CE spectrum was available. Similar to M2, M4 showed two chromatographic peaks with identical intensities. Hence, M4-1 and M4-2 were tentatively assigned as two diastereomers of 2′,7′-di-*S*-glutathionyl-5-CQA.

Bioactivation of 5-CQA in Human Liver S9 Fractions. When 5-CQA was incubated with NADPH- and GSH-supplemented human liver S9 fractions, the metabolic profiles were the same as those in the HLM (Fig. 8A). The addition of SAM to the incubations additionally resulted in three methylated metabolites (M6-1, M6-2, and M6-3) and four methylated GSH conjugates (M7-1, M7-2, M7-3, and M7-4), as shown in Fig. 8B and Table 1.

The LC retention times of M6-1, M6-2, and M6-3 were 18.3, 19.1, and 19.5 min, respectively. They gave the same deprotonated molecules at *m/z* 367.103, which was 14.020 Da higher than that of 5-CQA, indicating methylation. According to a previous study (Kuhnert et al., 2010), all of the acyl isomers of methylated 5-CQA (feruloylquinic and isoferuloylquinic acids) can be readily distinguished by their distinct tandem MS spectra in the negative ion mode. In the current study, the high CE spectra of three metabolites were significantly different. The base peak at *m/z* 191.053 without other obvious fragment ions was observed for M6-1, suggesting that it was 5-*O*-feruloylquinic acid (5-FQA). For M6-2 and M6-3, the base peaks were both at *m/z* 173.043. However, M6-2 produced a secondary fragment ion at *m/z* 111.046 and M6-3 produced a secondary fragment ion at *m/z* 193.052. By a direct comparison of the ion species and intensities in the spectra with literature (Kuhnert et al., 2010), M6-2 and M6-3 were tentatively identified as 5-*O*-isoferuloylquinic acid (5-iFQA) and 4-*O*-feruloylquinic acid (4-FQA), respectively.

The LC retention times of M7-1 to M7-4 were 11.3, 11.8, 12.7, and 13.3 min, respectively. They possessed the same deprotonated mole-

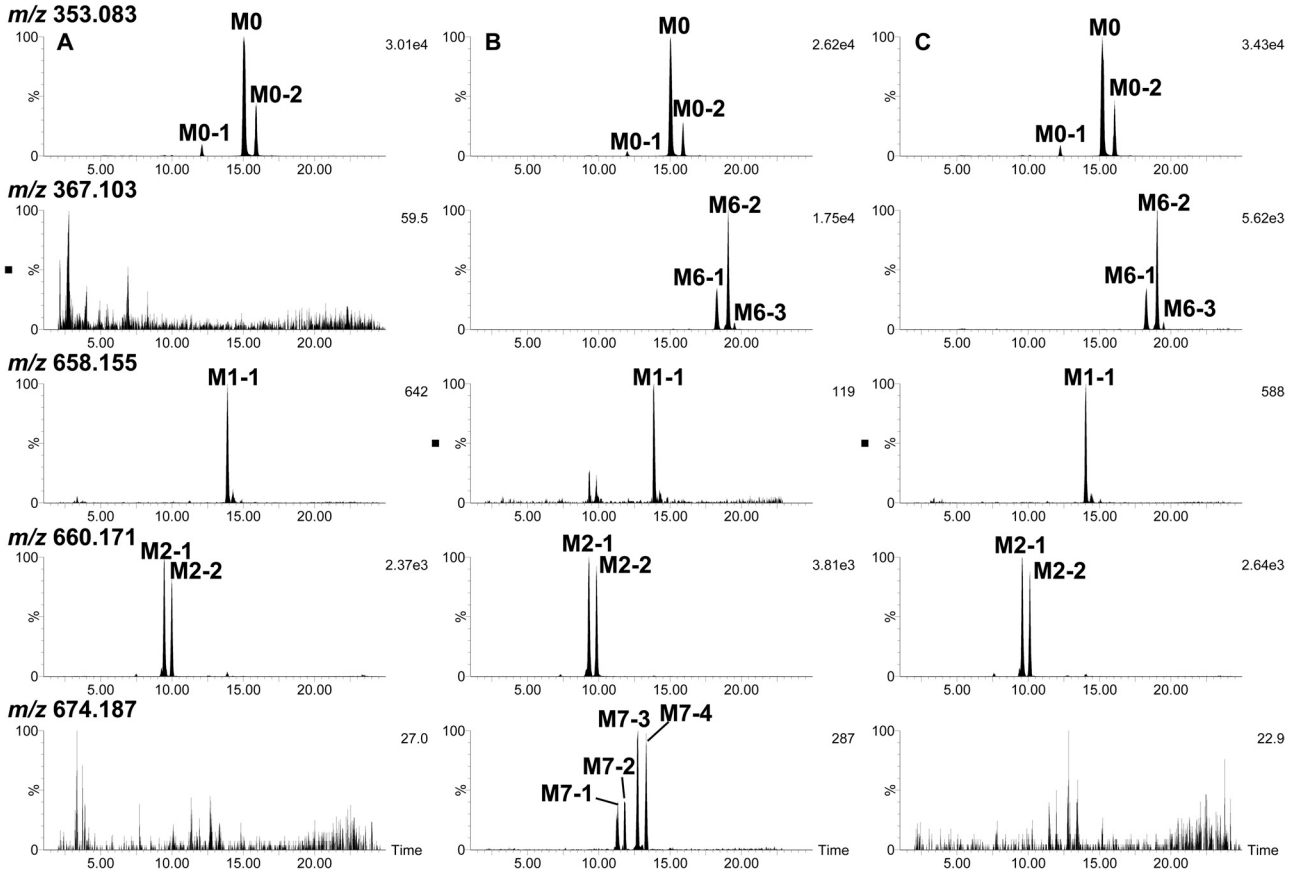

FIG. 8. Extracted ion chromatograms of 5-CQA and its metabolites formed in human liver S9 fractions incubations: supplemented only with GSH (A); supplemented with SAM and GSH (B); and supplemented with COMT inhibitor, SAM, and GSH (C).

cules at *m/z* 674.187, consistent with the attachment of the glutathionyl moiety (307.084 Da) to the methylated metabolites (M6). The loss of methylated 5-CQA moiety led to a predominant ion at *m/z* 306.084 in the high CE spectra of M7-1 to M7-4, similar to the exocyclic GSH conjugates M2-1 and M2-2. This finding indicated that M7-1 to M7-4 were formed by the 1,4-addition of one GSH to the α,β-unsaturated carbonyl group of M6-1 and M6-2 at C-7′. To explore this hypothesis, M6-1 and M6-2 were isolated from a scaled-up human liver S9 fraction reaction with 5-CQA, and then sequentially incubated with a mixture of M6-1 and M6-2 with GSH. The synthesized 7′-SG-5-CQA was also incubated with SAM-supplemented human liver S9 fractions. As expected, M7-1 to M7-4 were detected in both incubations. The product ion at *m/z* 191.057 was also obvious for M7-1 and M7-2, whereas the product ion at *m/z* 173.048 was obvious for M7-3 and M7-4. Hence, we speculated that M7-1 and M7-2 were two diastereomers of 7′-*S*-glutathionyl-5-*O*-feruloylquinic acid, and M7-3 and M7-4 were two diastereomers of 7′-*S*-glutathionyl-5-*O*-isoferuloylquinic acid.

The addition of SAM to the NADPH- and GSH-supplemented human liver S9 fractions with 5-CQA led to an 80% decline in the formation of the ring GSH conjugate M1-1. However, after the inhibition of COMT activity by tolcapone, the formation of M1-1 was increased four times (Table 2). This observation indicated that O-methylation may potentially circumvent the oxidative capability of 5-CQA to its electrophilic *ortho*-benzoquinone.

Identification of 5-CQA-Derived GSH Conjugates in Rat Plasma. To further investigate whether oxidative bioactivation occurs in vivo, the circulating metabolic profiles of 5-CQA in rats were examined. After an intravenous injection of 11 mg/kg 5-CQA, a total of 12 metabolites was discovered in plasma, in addition to the parent drug and its acyl-isomer (M0-2). These metabolites can be classified into five main types, including methylated (M6-1 and M6-2, *m/z* 367.102), sulfated (M8-1, M8-2, and M8-3, *m/z* 433.045), methylated and sulfated (M9-1, M9-2, and M9-3, *m/z* 447.059), glucuronidated (M10-1 and M10-2, *m/z* 529.121), as well as methylated and glucuronidated (M11-1 and M11-2, *m/z* 543.136) metabolites. No GSH conjugate derived from 5-CQA was detected. However, when the rats were pretreated with the COMT inhibitor tolcapone before 5-CQA injection, the methylated metabolites significantly decreased, whereas the ring GSH conjugate M1-1, identical with that observed in the HLM incubation studies, was detectable. All of these results supported the finding that O-methylation and *ortho*-benzoquinone metabolite formation are two competing pathways for 5-CQA. In addition, when a nonspecific P450 inhibitor ABT was intraperitoneally administered to rats simultaneously with the tolcapone dosing before the injection of 5-CQA, the GSH conjugate M1-1 disappeared in the circulation, indicating that the formation of M1-1 was mediated by P450s.

The metabolism of 5-CQA was investigated in LPS-induced inflammatory rats. Not surprisingly, the GSH conjugate M1-1 was also detected in plasma, and its formation was expected to be catalyzed by MPO released by leukocytes.

The extracted ion chromatograms of M1-1 in rat plasma are shown in Fig. 9. Information on the metabolites identified in the rat plasma is summarized in Table 3.

Discussion

5-CQA is widely distributed in daily diet and medicinal herbs. Due to its high hydrophilicity, 5-CQA cannot be absorbed directly in the

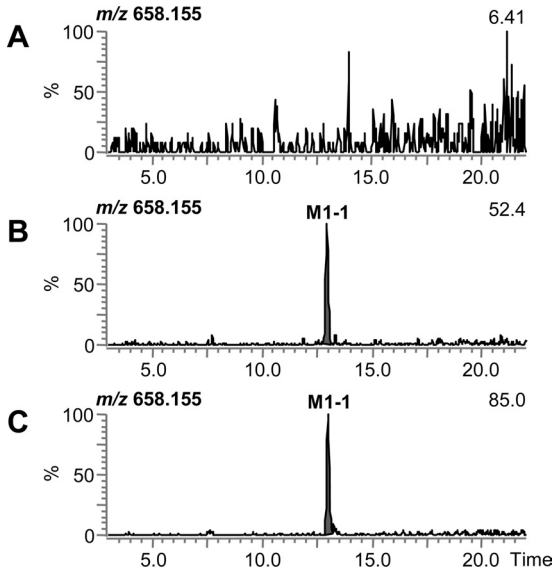

FIG. 9. Extracted ion chromatograms of M1-1 in the plasma of normal rats (A), COMT activity-inhibited rats (B), and LPS-induced inflammation rats (C).

gastrointestinal tract as intact molecule, and only a trace portion of 5-CQA could be hydrolyzed to its aglycone form caffeic acid by intestinal bacterial, then absorbed (Azuma et al., 2000; Dupas et al., 2006). Although caffeic acid can undergo analogous bioactivation pathways as 5-CQA, the limited amount of caffeic acid in vivo is supposed to be readily handled by the GSH pool in the liver and, alternatively, by O-methylation, glucuronidation, as well as sulfation. Thus, 5-CQA is relatively safe when taken orally. However, when it is used intravenously, its plasma concentration is very high and may exceed a threshold for eliciting a toxicological response. During the last decade, several herbal injections containing 5-CQA have been widely used in China, and some allergic as well as hepatotoxic responses have been reported (Li et al., 2010; Zhang et al., 2010). These herbal injections are mainly used to treat common colds, upper respiratory tract infections, cardiovascular diseases, and cancers. The target patients are believed to have different degrees of inflammation or oxidative stress, which may alter the metabolism and bioactivation pathways of 5-CQA. The current study mainly focused on characterizing the bioactivation pathways of 5-CQA, as well as investigating the impacts of different pathological situations and COMT activity on the bioactivation of 5-CQA.

Multiple GSH conjugates were identified after adding the nucleophilic agent GSH to each incubation system. The results of the UPLC/Q-TOF MS and/or NMR experiments implied that these GSH conjugates can be mainly formed by two metabolic pathways, as depicted in Scheme 1. One pathway is oxidation of the catechol moiety to *ortho*-benzoquinone intermediate, which can be trapped by GSH to form ring GSH conjugates (M1-1–M1-4, M3, and M5). The other pathway is 1,4-addition of GSH directly to the C-7′ position of the α,β-unsaturated carbonyl group of the parent compound, leading to the formation of exocyclic GSH conjugates (M2-1 and M2-2). The former pathway was found to require the presence of enzymes, and the latter proceeded in a nonenzymatic manner but could be accelarated by cytosolic GST. These findings demonstrated the high reactivities of 5-CQA to the nucleophiles, and understanding the bioactivation pathways of 5-CQA as well as their potential links to its toxicity are important.

The results obtained from the HLM experiments proved that P450 enzymes can catalyze the oxidation of 5-CQA to *ortho*-benzoquinone. Isoform profiling using individual recombinant human P450s and specific chemical inhibitors suggested that 3A4 and 2E1, relative to other major P450 isoforms, primarily mediated the formation of this reactive intermediate. M1-1 was also detected in the CHP-supplemented HLM incubations. In general, P450s supplemented with NADPH act as a monooxygenase in catalyzing the two-electron oxidation of a variety of substrates to quinones, whereas in the absence of NADPH or oxygen, P450 can use H_2O_2 or lipid peroxides to catalyze the single-electron oxidation of substrates to semiquinone radicals, which then transform into quinones (Tafazoli and O'Brien, 2005). The present experiments provided clear evidence that 5-CQA can be metabolically activated by both P450 monooxygenase and peroxidase activities. Oxidative stress may also enhance the production of the *ortho*-benzoquinone intermediate of 5-CQA because a 6-fold increase in M1-1 formation was observed in the CHP-supplemented HLM, compared with that in the NADPH-supplemented HLM.

MPO has been known to provide an alternative to P450-mediated bioactivation for a number of substrates with low redox potentials (Pattison and Davies, 2006). MPO is most abundantly expressed in activated mammalian leukocytes, including neutrophils and monocytes, or, to a lesser extent, in tissue macrophages such as Kupffer

TABLE 3

Metabolite data for 5-CQA in rat plasma (15 min after dosing)

No.	Description	Retention Time	Formula	Calculated Mass	Measured Mass	Relative Mass Response		
						5-CQA	5-CQA + LPS	5-CQA + Tolcapone
		min		$[M+H]^+$			%	
M0	5-CQA	14.0	$C_{16}H_{18}O_9$	353.083	353.085	16.9	15.1	18.3
M0-2	4-CQA	14.6	$C_{16}H_{18}O_9$	353.082	353.085	0.4	0.4	0.5
M1-1	2′-SG-5-CQA	13.0	$C_{26}H_{33}N_3O_{15}S$	658.155	658.155	–	0.2	0.2
M6-1	5-FQA	16.4	$C_{17}H_{20}O_9$	367.100	367.102	5.2	3.5	3.1
M6-2	5-iFQA	17.0	$C_{17}H_{20}O_9$	367.102	367.102	4.1	2.5	2.9
M8-1	Sulfate conjugate of 5-CQA	17.2	$C_{16}H_{18}O_{12}S$	433.046	433.045	1.1	2.8	4.6
M8-2	Sulfate conjugate of 5-CQA	19.0	$C_{16}H_{18}O_{12}S$	433.043	433.044	10.9	26.9	39.4
M8-3	Sulfate conjugate of 4-CQA	19.7	$C_{16}H_{18}O_{12}S$	433.038	433.041	0.3	0.5	–
M9-1	Sulfate conjugate of 5-FQA	18.0	$C_{17}H_{20}O_{12}S$	447.058	447.059	30.5	24.5	14.9
M9-2	Sulfate conjugate of 4-FQA	19.1	$C_{17}H_{20}O_{12}S$	447.056	447.058	0.7	0.6	–
M9-3	Sulfate conjugate of 5-iFQA	19.8	$C_{17}H_{20}O_{12}S$	447.062	447.061	26.2	20.4	14.0
M10-1	Glucuronide conjugate of 5-CQA	11.2	$C_{22}H_{26}O_{15}$	529.124	529.122	–	0.2	0.2
M10-2	Glucuronide conjugate of 5-CQA	13.9	$C_{22}H_{26}O_{15}$	529.118	529.119	1.2	1.6	1.4
M11-1	Glucuronide conjugate of 5-FQA	12.0	$C_{23}H_{28}O_{15}$	543.137	543.136	–	0.1	–
M11-2	Glucuronide conjugate of 5-iFQA	14.6	$C_{23}H_{28}O_{15}$	543.131	543.133	0.8	0.8	0.5

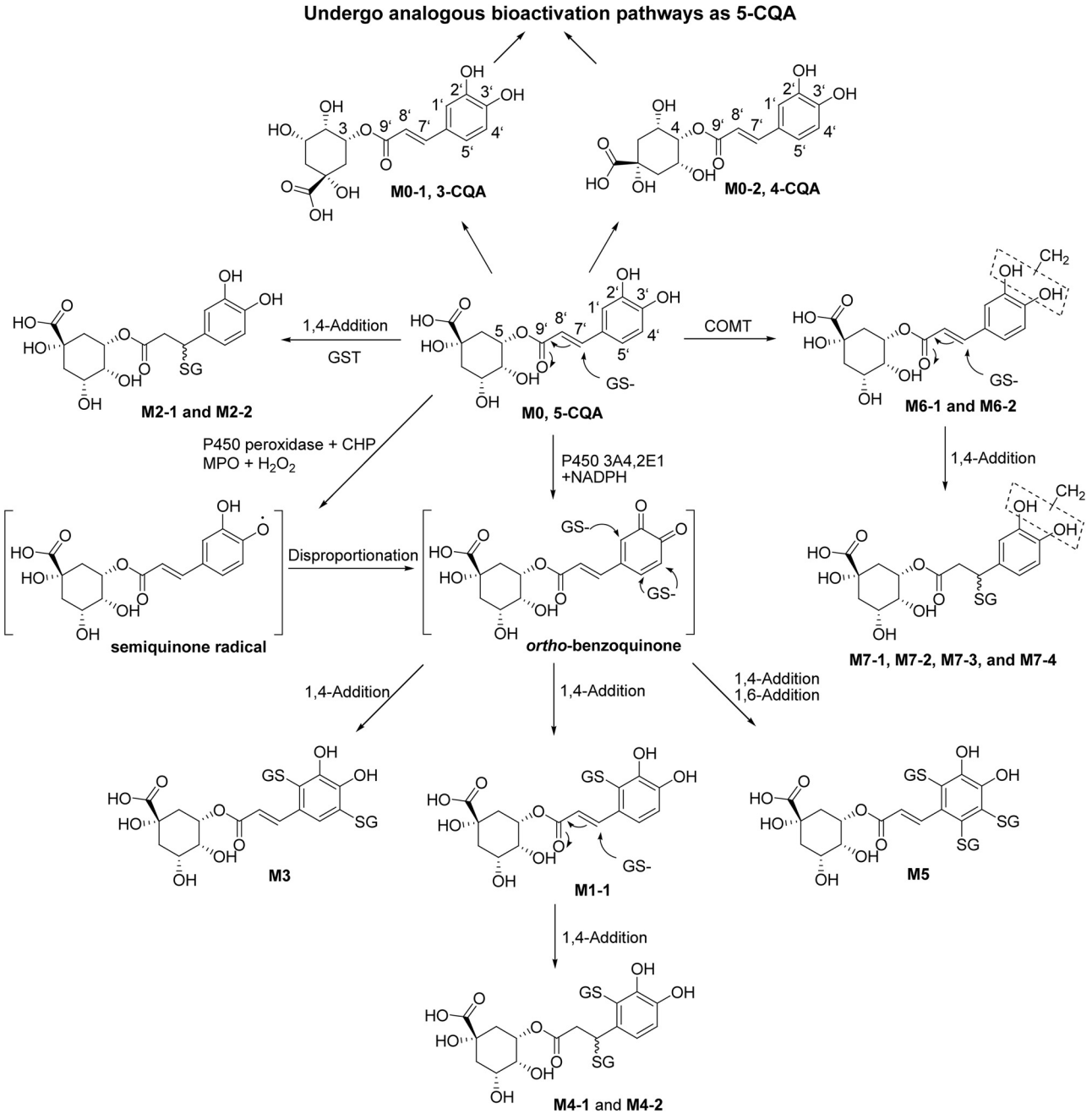

SCHEME 1. Proposed mechanism of bioactivation and GSH conjugate formation of 5-CQA.

cells (resident macrophages of the liver). These cells become activated during inflammation. Numerous drugs that have been withdrawn from the market because of hepatotoxicity problems (e.g., troglitazone, tolcapone, mefenamic acid, and phenylbutazone) are markedly more toxic and pro-oxidant in human inflammatory disease models (Tafazoli et al., 2005). In the present experiment, 5-CQA was found to be bioactivated by MPO and PMA-activated human leukocytes. Greater amounts of M1-1 were also detected in the plasma of LPS-induced inflammatory rats. These results imply that of patients with inflammation, 5-CQA was more likely to be bioactivated by a single-electron oxidation mechanism to form radicals by MPO released from circulating activated leukocytes, thus inducing unwanted idiosyncratic reactions. However, the reactivity of the α,β-unsaturated carbonyl group did not change under different pathological situations.

Although the molecular mechanisms underlying the idiosyncratic toxicity remain unknown, several hypotheses have been proposed, including covalent protein binding and oxidative stress caused by reactive metabolites (Uetrecht, 2008). The current study proved that the *ortho*-benzoquinone metabolite of 5-CQA formed by P450 monooxygenase and other oxidizing enzymes was highly reactive. The α,β-unsaturated carbonyl group of 5-CQA itself was also electrophilic. Hence, 5-CQA was likely to alkylate cellular proteins in vivo in addition to the conjugation with GSH. Several research groups have shown that oxidized 5-CQA can react with lysine and cysteine residues in protein chains and form covalent-binding products in vitro (Hurrell and Finot, 1984; Gayen et al., 2008). Alternatively, the current experiment proved that 5-CQA can form semiquinone radical by P450 peroxidase and MPO, which can induce a redox cycle with

the corresponding *ortho*-benzoquinone. This phenomenon led to the formation of reactive oxygen species. Compelling evidence showed that reactive oxygen species can alter the redox state of cells or exert excessive oxidative stress on tissues (O'Brien, 1991; Bolton et al., 2000). A previous study has also pointed out that the hepatotoxicity of 5-CQA can be markedly increased when the peroxidase/H_2O_2 oxidation system was added to hepatocyte incubations (Moridani et al., 2001). Regardless of several research groups who have shown the antioxidative property of 5-CQA (Pari et al., 2010; Xu et al., 2010; Sato et al., 2011), the anti- and pro-oxidation properties of 5-CQA are not contradictory. The dose is critical with regards to the metabolic fate of the compound as well as metabolic switching and the route of administration. The α-tocopherol and troglitazone were demonstrated to be antioxidants, but their radical forms catalyzed by peroxidase at higher concentrations had undesirable pro-oxidant activities (Witting et al., 1999; Tafazoli et al., 2005).

In vitro incubation of xenobiotics with cofactors that only support P450 or peroxidase activity can be misleading in bioactivation capability assessments because the phase II metabolism enzymes are not included. Catechols have been shown to be good substrates for COMT, UDP-glucuronosyltransferases, and sulfotransferases, which can potentially diminish the oxidation pathway to electrophilic quinones (Taskinen et al., 2003; Chen et al., 2011). This phenomenon was observed in the current analysis. When SAM was included in human liver S9 incubations, the major metabolites were methylated 5-CQAs (M6-1 and M6-2), with only a small amount of M1-1 detected. However, the formation of M1-1 increased by four times after tolcapone inhibited COMT activity. Similar phenomena were also observed in the metabolism study in rats. The major metabolic pathways were methylation, sulfation, and glucuronidation in rats only given 5-CQA injections and no GSH conjugate of 5-CQA was formed. In contrast, M1-1 was detected in the COMT activity-inhibited rats. Taken together, these findings indicated that the O-methylation of 5-CQA in vivo may shield the oxidation of the catechol group to *ortho*-benzoquinone. It is reasonable to surmise that glucuronidation and sulfation have similar effects. Consequently, high levels of 5-CQA bioactivation can be expected when 5-CQA-related herbal injections are prescribed to patients with low phase II enzyme activities.

In conclusion, the current study demonstrated that 5-CQA was bioactivated by P450 monooxygenases (mainly 3A4 and 2E1) and peroxidases (P450 peroxidase and MPO) to an *ortho*-benzoquinone intermediate, which was attacked by GSH to form mono-, di-, and tri-GSH conjugates. Under normal conditions, the competing O-methylation of 5-CQA may prevent the catechol group from oxidizing into *ortho*-benzoquinone. However, under oxidizing or inflammatory or COMT activity-inhibited conditions, 5-CQA may be more susceptible to facile bioactivation to reactive *ortho*-benzoquinone species. 5-CQA itself could also directly react with GSH at the C-7′ position of the α,β-unsaturated carbonyl group, which could be accelerated by cytosolic GST. The present study is the first report on the nature of the ring and exocyclic GSH conjugates of 5-CQA. The results have expanded understanding on the bioactivation of 5-CQA under different situations. The potential safety issues regarding 5-CQA-related herbal injections need further evaluation because the different pathological situations and phase II enzyme (e.g., COMT) activities of patients may alter the bioactivation extent of 5-CQA and result in unexpected toxicities.

Acknowledgments

We thank Dr. Tao Yuan for the synthesis and purification of standard compounds; Dr. Liang Li for conducting the NMR analysis of GSH conjugates; Hua Li for help during microsomal incubations; and Chunying Gao for the helpful discussion.

Authorship Contributions

Participated in research design: Xie, Chen, and Zhong.

Conducted experiments: Xie.

Contributed new reagents or analytic tools: Xie and Chen.

Performed data analysis: Xie and Chen.

Wrote or contributed to the writing of the manuscript: Xie, Chen, and Zhong.

References

Azuma K, Ippoushi K, Nakayama M, Ito H, Higashio H, and Terao J (2000) Absorption of chlorogenic acid and caffeic acid in rats after oral administration. *J Agric Food Chem* **48:**5496–5500.

Bariana DS, Krupey J, Scarpati LM, Freedman SO, and Sehon AH (1965) Chlorogenic acid: further evidence for its antigenic and allergenic activity. *Nature* **207:**1155–1157.

Bolton JL, Trush MA, Penning TM, Dryhurst G, and Monks TJ (2000) Role of quinones in toxicology. *Chem Res Toxicol* **13:**135–160.

Chen Z, Chen M, Pan H, Sun S, Li L, Zeng S, and Jiang H (2011) Role of catechol-O-methyltransferase in the disposition of luteolin in rats. *Drug Metab Dispos* **39:**667–674.

Clifford MN (2000) Chlorogenic acids and other cinnamates - nature, occurrence, dietary burden, absorption and metabolism. *J Sci Food Agric* **80:**1033–1043.

Clifford MN, Johnston KL, Knight S, and Kuhnert N (2003) Hierarchical scheme for LC-MS^n identification of chlorogenic acids. *J Agric Food Chem* **51:**2900–2911.

Deng P, Zhong D, Nan F, Liu S, Li D, Yuan T, Chen X, and Zheng J (2010) Evidence for the bioactivation of 4-nonylphenol to quinone methide and ortho-benzoquinone metabolites in human liver microsomes. *Chem Res Toxicol* **23:**1617–1628.

dos Santos MD, Almeida MC, Lopes NP, and de Souza GE (2006) Evaluation of the anti-inflammatory, analgesic and antipyretic activities of the natural polyphenol chlorogenic acid. *Biol Pharm Bull* **29:**2236–2240.

Dupas C, Marsset Baglieri A, Ordonaud C, Tomé D, and Maillard MN (2006) Chlorogenic acid is poorly absorbed, independently of the food matrix: A Caco-2 cells and rat chronic absorption study. *Mol Nutr Food Res* **50:**1053–1060.

Freedman SO, Krupey J, and Sehon AH (1961) Chlorogenic acid: an allergen in green coffee bean. *Nature* **192:**241–243.

Gayen A, Chatterjee C, and Mukhopadhyay C (2008) GM1-induced structural changes of bovine serum albumin after chemical and thermal disruption of the secondary structure: a spectroscopic comparison. *Biomacromolecules* **9:**974–983.

Hurrell RF and Finot PA (1984) Nutritional consequences of the reactions between proteins and oxidized polyphenolic acids. *Adv Exp Med Biol* **177:**423–435.

Ji K, Chen J, Li M, Liu Z, Xia L, Wang C, Zhan Z, and Wu X (2009) Comments on serious anaphylaxis caused by nine Chinese herbal injections used to treat common colds and upper respiratory tract infections. *Regul Toxicol Pharmacol* **55:**134–138.

Jiang Y, Kusama K, Satoh K, Takayama E, Watanabe S, and Sakagami H (2000) Induction of cytotoxicity by chlorogenic acid in human oral tumor cell lines. *Phytomedicine* **7:**483–491.

Kuhnert N, Jaiswal R, Matei MF, Sovdat T, and Deshpande S (2010) How to distinguish between feruloyl quinic acids and isoferuloyl quinic acids by liquid chromatography/tandem mass spectrometry. *Rapid Commun Mass Spectrom* **24:**1575–1582.

Li BQ, Dong X, Yang GQ, Fang SH, Gao JY, Zhang JX, Gu FM, Miao XM, and Zhao H (2010) Role of chlorogenic acid in the toxicity induced by Chinese herbal injections. *Drug Chem Toxicol* **33:**415–420.

Moridani MY, Scobie H, Jamshidzadeh A, Salehi P, and O'Brien PJ (2001) Caffeic acid, chlorogenic acid, and dihydrocaffeic acid metabolism: glutathione conjugate formation. *Drug Metab Dispos* **29:**1432–1439.

Moridani MY, Scobie H, and O'Brien PJ (2002) Metabolism of caffeic acid by isolated rat hepatocytes and subcellular fractions. *Toxicol Lett* **133:**141–151.

O'Brien PJ (1991) Molecular mechanisms of quinone cytotoxicity. *Chem Biol Interact* **80:**1–41.

Panzella L, Napolitano A, and d'Ischia M (2003) Oxidative conjugation of chlorogenic acid with glutathione. Structural characterization of addition products and a new nitrite-Promoted pathway. *Bioorg Med Chem* **11:**4797–4805.

Pari L, Karthikesan K, and Menon VP (2010) Comparative and combined effect of chlorogenic acid and tetrahydrocurcumin on antioxidant disparities in chemical induced experimental diabetes. *Mol Cell Biochem* **341:**109–117.

Pattison DI and Davies MJ (2006) Reactions of myeloperoxidase-derived oxidants with biological substrates: gaining chemical insight into human inflammatory diseases. *Curr Med Chem* **13:**3271–3290.

Rodrigues AD (1999) Integrated cytochrome P450 reaction phenotyping: attempting to bridge the gap between cDNA-expressed cytochromes P450 and native human liver microsomes. *Biochem Pharmacol* **57:**465–480.

Sato Y, Itagaki S, Kurokawa T, Ogura J, Kobayashi M, Hirano T, Sugawara M, and Iseki K (2011) In vitro and in vivo antioxidant properties of chlorogenic acid and caffeic acid. *Int J Pharm* **403:**136–138.

Shibata H, Sakamoto Y, Oka M, and Kono Y (1999) Natural antioxidant, chlorogenic acid, protects against DNA breakage caused by monochloramine. *Biosci Biotechnol Biochem* **63:**1295–1297.

Tafazoli S and O'Brien PJ (2005) Peroxidases: a role in the metabolism and side effects of drugs. *Drug Discovery Today* **10:**617–625.

Tafazoli S, Spehar DD, and O'Brien PJ (2005) Oxidative stress mediated idiosyncratic drug toxicity. *Drug Metab Rev* **37:**311–325.

Taskinen J, Ethell BT, Pihlavisto P, Hood AM, Burchell B, and Coughtrie MW (2003) Conjugation of catechols by recombinant human sulfotransferases, UDP-glucuronosyltransferases, and soluble catechol O-methyltransferase: structure-conjugation relationships and predictive models. *Drug Metab Dispos* **31:**1187–1197.

Uetrecht J (2008) Idiosyncratic drug reactions: past, present, and future. *Chem Res Toxicol* **21:**84–92.

Witting PK, Mohr D, and Stocker R (1999) Assessment of prooxidant activity of vitamin E in human low-density lipoprotein and plasma. *Methods Enzymol* **299:**362–375.

Xie C, Yu K, Zhong D, Yuan T, Ye F, Jarrell JA, Millar A, and Chen X (2011a) Investigation of isomeric transformations of chlorogenic acid in buffers and biological matrixes by ultraperformance liquid chromatography coupled with hybrid quadrupole/ion mobility/orthogonal acceleration time-of-flight mass spectrometry. *J Agric Food Chem* **59:**11078–11087.

Xie C, Zhong DF, and Chen XY (2011b) [Metabolites of injected chlorogenic acid in rats.] *Yao Xue Xue Bao* **46:**88–95.

Xu Y, Chen J, Yu X, Tao W, Jiang F, Yin Z, and Liu C (2010) Protective effects of chlorogenic acid on acute hepatotoxicity induced by lipopolysaccharide in mice. *Inflamm Res* **59:**871–877.

Yan Z, Caldwell GW, and Maher N (2008) Unbiased high-throughput screening of reactive metabolites on the linear ion trap mass spectrometer using polarity switch and mass tag triggered data-dependent acquisition. *Anal Chem* **80:**6410–6422.

Zhang H, Li X, Zhou H, Xu X, and Chen W (2009) Determination of six phendic acids in mailuoning injection by RP-HPLC. *Chin J Info TCM* **16:**54–56.

Zhang N, Wang T, and Zhang H (2008) Determination of the content of chlorogenic acid in yinzhihuang injection by HPLC. *Mod Med & Health* **24:**2553–2554.

Zhang R, Tang N, Lin H, Ma J, Xie C, and Chen X (2010) Allergenicity assessment and comparison between chlorogenic acid and shuanghuanglian fenzhenji. *World Sci Technol* **12:**1005–1008.

Address correspondence to: Dr. Xiaoyan Chen, Shanghai Institute of Materia Medica, Chinese Academy of Sciences, 501 Haike Rd., Shanghai 201203, China. E-mail: xychen@mail.shcnc.ac.cn